

Water quality parameters and phytoplankton characteristics in coastal mangrove ecosystem

Abstract

Studies on the water quality variable and phytoplankton characteristics in mangrove areas of Guangdong, China was carried out to determine the impact of changing water quality on phytoplankton and its cell size characteristics. Plankton samples were collected spatially from July to August 2018, at 23 selected sites across the mangroves. From the 630 taxa identified, diatoms constituted the highest number of species (420 species) and contributed 71.90% of the total phytoplankton abundance. Other important phyla were Cyanobacteria (16.35%, with 83 species) and Chlorophyta (10.70%, with 87 species). Across all the sites, algal biomass was highest in the Coscinodiscophyceae compared to the other Classes of phytoplankton. Though the cell size range was 0.8-306 μm , a greater proportion of phytoplankton was found within > 1000 μm^3 and 250 to <100 μm^3 . The results of canonical correspondence analysis revealed that species with cell size <100 μm^3 were associated with increase electrical conductivity and nitrate concentration, while species with cell size >1000 μm^3 were associated with salinity and pH variation. The massive proliferation of these species, *Chaetoceros decipiens*, *Monoraphidium irregulare*, *Synechocystis* sp., and *Pseudanabaena limnetica* could become an indicator of nutrient enrichment. This study confirms that the Guangdong mangrove areas inhabit the richest phytoplankton community, and their cells size distributions are controlled by the water quality parameters.

Keywords: Algal biomass, cell-size dynamics, mangrove ecosystem, nutrients

Volume 14 Issue 1 - 2025

Aniefiok Ini Inyang, Monica Udeme Dan, Kokoette Sunday Effiong, Robert Udo Udo

Department of Marine Biology, Akwa Ibom State University, Ikot Akpaden, Nigeria

Correspondence: Aniefiok Ini Inyang, Department of Marine Biology, Akwa Ibom State University, Ikot Akpaden, Nigeria, Tel & Fax +234-904310-7269

Received: February 25, 2025 | **Published:** March 12, 2025

Introduction

Phytoplankton occupies an important component of the marine ecosystems, releasing oxygen during photosynthesis and aiding in the energy exchange process.¹ Its distribution and species abundance drive trophic state, productivity and energy flow in estuarine ecosystems.^{2,3} According to Sin et al.,⁴ phytoplankton community structure, composition, and species diversity in aquatic ecosystems are determined by several environmental variables. The spatial distribution of phytoplankton in the mangroves is widely affected by environmental variables such as water temperature, salinity, pH, electrical conductivity, turbidity, nutrient salts, and water calmness.^{5,6} The influence of these factors on the phytoplankton community alters the species composition and diversity.^{7,8} The mangrove ecosystem shows seasonal fluctuations among the environmental variables depending on regional rainfall, tidal inflow, and various abiotic and biotic processes.⁹

Usually, nutrient availability is considered as a key factor regulating phytoplankton composition, diversity, and structure, which reflects the environmental condition of the ecosystem.^{6,10,11} Phytoplankton community and size composition are known to be related to nutrient availability.¹² Changes in phytoplankton community composition are usually accompanied by changes in phytoplankton size distributions, which possibly affect zooplankton community composition and structure.¹² Since phytoplankton plays a very important role in the marine ecosystems, the study of phytoplankton communities is very important in the mangrove ecosystem.¹³⁻¹⁵ Recent studies have reviewed the factors regulating the diversity and community structure of phytoplankton in coastal ecosystems;^{5,6,16-20} but idealistically, phytoplankton abundance and community composition in the coastal mangroves of northern part of South China Sea received little attention.²⁰ The coastal waters of Guangdong Province, China have received a large amount of nutrients and other pollutants from

ivers and their watersheds²¹ that can affect the spatial dynamic of the phytoplankton community structure.

Therefore, it is important to investigate the relationship between changes in nutrients concentration and phytoplankton community characteristics in coastal mangrove ecosystem of Guangdong Province, China. It's in this light that we elucidate the phytoplankton composition, cell-size dynamics, and biomass production across the mangroves during the rainy season.

Study area

The sampling was done at 23 different locations throughout the Guangdong mangrove forests, at latitude 20°12'-25°31'N and longitude 109°45'-117°20' E (Figure 1). The sampling sites were characterized by different species of true mangroves, such as *Acrostichum aureum*, *Excoecaria agallocha*, *Bruguiera gymnorrhiza*, *Kandelia obovata*, *Rizophora stylosa*, *Lumnizera racemosa*, *Aegicera corniculatum*, *Avicennia marina*, and *Acanthus ilicifolius*, and non-true mangrove species e.g. *Pongamia pinnata*, *Hibiscus tiliaceus*, *Thespesia populnes*, *Herliera littoralis*, *Cerbera manghas*, *Clerodendrum inerme*, and *Pluchea indica*.⁶ Guangdong mangroves are influenced by semidiurnal to mixed tides all year round, with a tidal range of 0.8 m (neap tides) to 4.0m (spring tides). The average annual precipitation in the study region is ~2,000mm,²² and about 85% of the total rainfall is concentrated in the wet season (April to September).

Materials and methods

Sampling procedures

The sample collection was carried out across the 23 sites inside the mangroves between July and August 2018. At each site, measurement of environmental variables and collection of plankton samples were obtained during flood tide.

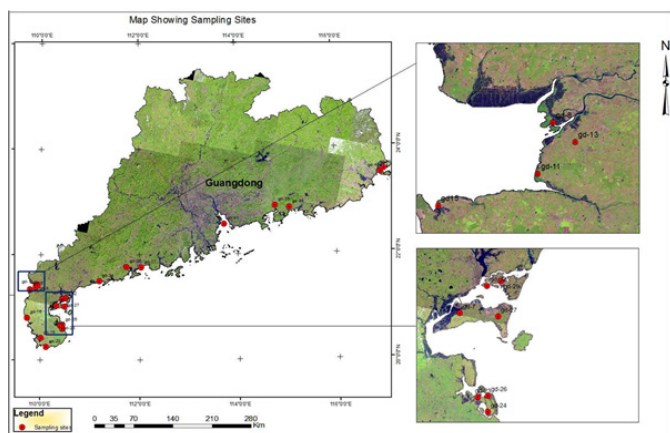


Figure 1 Map of the study area.

Plankton sampling and laboratory procedures

The phytoplankton samples were collected during flooding tide by vertically hauling within the depth of 1m, using plankton net of 0.045mm size. Approximately 90 L of water was filtered at each station, and the net was rinsed before new sampling to avoid contamination of the new sample by the previous one. The collected phytoplankton samples in 300mL plastic bottles were preserved with neutral Lugol’s solution of 10% for further analysis. Further analysis and identification were conducted as described by Inyang and Wang.⁶ The phytoplankton photographs were taken using Olympus DP73 digital cameras at the magnification level of 400X and 200X. All organisms, unicells, filaments, trichomes, or coenobia were counted as a single algal unit and recorded as cells.ml⁻¹. At least 500cells were counted at each station. The cell count was converted from cells.ml⁻¹ of phytoplankton into cells/liter of cell density according to the equation:

$$\text{Cell density (Cell.L}^{-1}\text{)} = \frac{(A \times 1000)V}{L} \dots\dots\dots (1)$$

Where;

A = Average number of cells count in the S-R counting chamber

V = volume of plankton concentrates (50mL)

L = Volume of original water filtered in a liter (90L).

The phytoplankton species identification up to the species level was based on the morphological structure of the cell, using the following literatures²³⁻²⁶ and with the following noted website, algaebase.com (ab), World Register of Marine Species (WoRMS), Protist information server of Japan (<http://protist.i.hosei.ac.jp>), microscopyview.com and Nordic Microalgae. However, the phytoplankton taxonomy was carried out using.²⁷

Algal biovolume determination

During the counting process, each species was allocated to size classes following Olenina et al.,²⁸ The descriptions of the cell volume are based on the measures of the size of the species and the adaptation of the shapes to geometric shapes as described by Olenina et al.,²⁸ and, Sun and Liu.²⁹ The individual biovolumes of the different counting units were then multiplied with their respective abundance to get the biovolume per L, according to the equation:

$$\text{Biovolume taxon } (\mu\text{m}^3.\text{L}^{-1}) = \text{abundance (L}^{-1}\text{)} \times \text{VCU} \times 10^{-9} \dots\dots\dots (2)$$

Where; VCU = volume of counting unit (μm³)

From the biovolume data, the biomass (wet weight) was juxtaposed by rough assumption of a plasma density of 1 g.cm⁻³ according to Cen:³⁰

$$10^6 \mu\text{m}^3.\text{L}^{-1} \text{ (biovolume)} = 1 \mu\text{g}.\text{L}^{-1} \text{ (wet weight)} \dots\dots\dots (3)$$

The biovolume classes adopted in this work is given below:

Very small = < 100μm³; Small = 100 – 250μm³; Medium-sized = 250 – 1000μm³; Large and very large = > 1000 μm³.^{31,32}

Measurement of water quality variables

At each site, in-situ measurement of water quality parameters such as water temperature, pH, salinity, electrical conductivity (EC), turbidity, and total dissolved solids (TDS) were measured using a Quanta® Water Quality Monitoring System (Hydrolab Corporation, USA) during flood water level within the depth of 1m. 300mL of surface water was collected using sampling plastic bottles for analysis of nutrients (phosphate, nitrate, nitrite and silicate). The water sample was filtered using 0.22 μm Whatman® GF/F filters before analysis. Within 2–3hrs after sampling, nitrate (NO₃-N), nitrite (NO₂-N), phosphate (PO₄-P), and silicate (SiO₃-Si) were analyzed using a SKALAR auto-analyzer (Skalar Analytical B.V. SanPlus, Holland). Chlorophyll *A* analysis was carried out according to HELCOM³³ using a SHIMADZU Spectrophotometer (UV-1700-Japan) and calculated as follows:

$$Cv = \frac{10^3 \cdot e \cdot A(665K)}{83 \cdot V \cdot L} \dots\dots\dots (4)$$

Where;

Cv = Chl. *A* concentration, mg/m³,

e = volume of ethanol, cm³

A(665K) = absorbance at 665nm (the peak) minus the absorbance at 750nm after correction by the cell-to-cell blank, L = length of the curvette, (cm), V = water volume filtered, dm³, 83 = absorption coefficient in 96% ethanol.

Rainfall data was acquired from the Global Precipitation Climatology Project (GPCP) during the southwest monsoon period (April to September, 2018). The total value of July and August precipitation data was used in the analysis.

Data analysis

Statistical analysis was carried out with the aid of SPSS (version 22.0), Canoco 5, PAST v. 3, and PRIMER v.7. To estimate the significant factor among the water quality parameters in the mangrove forests, PCA plot³⁴ was carried out via Canoco 5 software (Houston, TX, USA) on the eleven water quality variables. The variation in the water quality variables between the sites was studied by ANOVA (one-way) with the Duncan test at a probability level of 5%, comparing the mean value of variable with significant F between the sites. Before this analysis, all the water quality variables were transformed with Log(X + 1) (except pH) and tested for normality test through kurtosis and skewness statistical tests (p < 0.001).

The phytoplankton community structure was analyzed using non-parametric multivariate tools, found in PRIMER v. 7 (PRIMER-E Ltd, Rorborough, Plymouth, UK) software package in accordance with Clarke and Warwick,³⁵ Clarke and Gorley.³⁶ Before multivariate analysis, all species that occurred in less than five sites and/or

that never surpassed, at least in one sample, 0.5% of abundance were discarded to reduce the influence of rare taxa. Meanwhile, all the multivariate analysis (Cluster, SIMPER, and metric Multi-Dimensional Scaling) was based on the $\text{Log}(X + 1)$ pre-transformed original data matrix. The SIMPER routine was performed to calculate the average similarity of the samples of each site, but also the average dissimilarity of all pairs of inter-site samples based on the grouping factor generated by the cluster analysis.

However, for better visualization of the Bray-Curtis similarity matrix in a two-dimensional plot, a non-metric Multi-Dimensional Scaling (nMDS) ordination was performed. The distances between pairs of samples in the plot reflect their relative dissimilarity in species composition and abundance. Meanwhile, the nMDS ordination plot was tested for significant differences between groups of samples, using one-way analysis of similarities (ANOSIM),³² in PRIMER v. 7 (PRIMER-E Ltd, Roborough, Plymouth, UK).

To assess the relationships between nutrients and phytoplankton cell sizes, canonical correspondence analysis (CCA) using PAST v. 3 and Pearson's correlation analysis (SPSS 22.0) were employed.

Results

Spatial variation in environmental parameters

The spatial distribution of the environmental variables across the mangroves is presented in Table S1 (supplementary material). The univariate statistics of the environmental variables and their normality test are given in Table 1. The test results confirm the normal distribution of the data (pH, tds, EC, turbidity, salinity, water temperature, reactive phosphate, and silicate) with a confidence coefficient of 95% ($p < 0.05$). Moreover, the results of the ANOVA and post hoc (Duncan) tests ($p < 0.05$) provided in Table S2 (supplementary material) confirmed that all the environmental variables were significantly different across the sampling sites due to the differences in the catchment characteristics. As shown in Table S3 (supplementary material), precipitation has a small positive impact on nitrate, EC, turbidity, and chlorophyll *A* concentration, but a significant impact on the water temperature ($p < 0.05$). Chlorophyll *A* concentration varied greatly across the sampling sites, with a mean value of $1.82 \text{ mg}\cdot\text{m}^{-3}$. Its highest value was $13.53 \text{ mg}\cdot\text{m}^{-3}$ (gd-11), while its lowest value was $0.14 \text{ mg}\cdot\text{m}^{-3}$ (gd-20). It was noted that the chlorophyll *A* concentration was higher across the Leizhou Peninsula (i.e. gd-2 to gd-29) than in other places in the mangroves.

Table 1 Descriptive statistics and normality test ($p < 0.05$) of the physiochemical variable measured across the mangrove forest ($n = 23$)

Variables	pH	Tds (ppt)	Salinity	Turb. (FTU)	Tem (°C)	EC ($\mu\text{g}/\text{sm}$)	Phosp. (mg/L)	Nitrate (mg/L)	Nitrite (mg/L)	Silicate (mg/L)	Chl. A (mg/m^3)
Min	7.47	2.04	2.15	9.20	12.79	86.90	0.00	0.00	0.00	1.01	0.14
Max	8.71	22.02	22.82	204.00	34.49	9702.00	2.50	2.00	1.75	3.04	13.53
Mean	8.04	11.26	13.44	56.84	29.24	3472.78	1.09	0.09	0.14	2.16	1.90
Stand. Dev.	0.39	6.14	7.46	42.42	4.32	2022.02	1.05	0.42	0.47	0.41	2.80
Variance	0.15	37.70	55.69	1799.14	18.63	4088562.14	1.11	0.17	0.22	0.17	7.84
Skewness	-0.03	-0.68	-0.67	-0.34	-0.66	-0.22	0.13	3.43	3.26	0.37	1.77
Kurtosis	-1.23	-1.13	-1.14	0.64	1.61	-0.08	-1.86	11.38	9.72	0.24	3.99

Principal component analysis (PCA) given in Figure 2 produced four principal components that cumulatively explained 88.18% of water quality variations between the sites, with axis1 (42.41%) and axis 2 (21.80%) with eigenvalues of 0.42 and 0.21 respectively. The total variation was 67.05% with Tau value as 0.51 at the eigenvalues of 1 of the variation between the sites. Meanwhile, variables such as, EC, temperature, turbidity, salinity/tds, nitrite, and silicate contributed significantly to the water quality variability in the mangroves. Also, phosphate and nitrate contributed averagely.

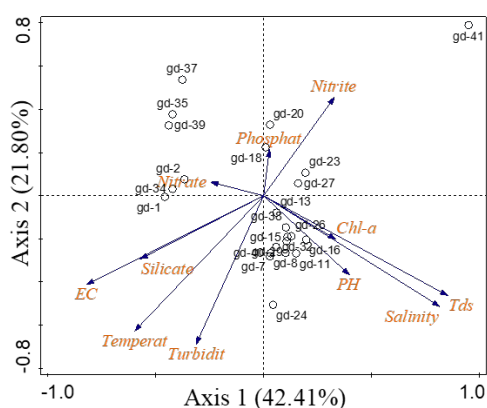


Figure 2 The PCA biplots of the environmental variables in the mangrove ecosystems [EC. electrical conductivity, Tds. total dissolve solids, Chl. A chlorophyll A].

Phytoplankton taxa and biomass distribution

A total of 630 taxa belonging to 13 Classes of phytoplankton were identified across the 23 studied sites, Table S4 (supplementary material). The present distribution of the identified taxa was classified into 5 groups: rare (32.22% of the total taxa identified), less common (38.73%), common (18.25%), abundant (5.08%) and very abundant (5.71%). Meanwhile, the following species were reported most common and abundant species in the mangroves, *Coscinodiscopsis jonesiana*, *Cyclotella meneghiniana*, *Skeletonema costatum*, *Bacillaria paxillifer*, *Nitzschia palea*, and *Navicula cryptonella* (Figure 3). Spatially, diatoms (with 420 species) represented 71.90% of the total phytoplankton biomass. Other groups recorded were Cyanophyta (16.35%, with 83 species including 24 new taxa) and Chlorophyta (10.70%, with 87 species including 37 new taxa); Dinopyta, Euglenophyta, Charophyta, Orcharophyta, and Cryptophyta constituted $< 0.5\%$ of the total phytoplankton abundance, Figures S1&S2 (supplementary material). The spatial distribution of phytoplankton Classes found in the mangroves are given in Figure 4a. Diatom – Mediophyceae such as *Chaetoceros* sp., *C. meneghiniana*, *Thalassiosira mala*, *T. leptopus*, *T. minicosmica*, and *S. costatum* were the main predominant species found across the Leizhou Peninsula (gd-7, 15, 23, 24, 26, 27, 29). A shift from the Mediophyceae dominating assemblage to the Bacillariophyceae dominating assemblage was observed across gd-1, 8, 20, 32, 38 & 40. Precisely, *Asterionellopsis glacialis*, *N. longissima* var. *reversa*, and *Thalassionema nitzschioides* predominated gd-20; *N. sigma*, *N.*

palea, and *N. cryptonella* predominated gd-8; and *N. brevissima*, *N. clausii*, and *Cocconeis placentula* predominated gd-32, 38 & 40. High abundance of Coscinodiscophyceae was only observed at gd-13 & 15, where *C. jonesiana* proliferates the surface water. Cyanophyta such as the periphytic taxa (*Oscillatoria* sp.) and planktonic taxa

(*Merismopedia* sp., *Synechococcus* sp., *Pseudanabaena limnetica* & *Anabaenopsis elenkinii*) proliferate the surface water across gd-2, 16 & 18. Also, planktonic cyanobacteria such as *Aphanocapsa* sp., *Microcystis* sp., *Chroococcus* sp. & *Synechocystis* sp. proliferate the surface water at site gd-34, 35, 37 & 41(Figure 4a).

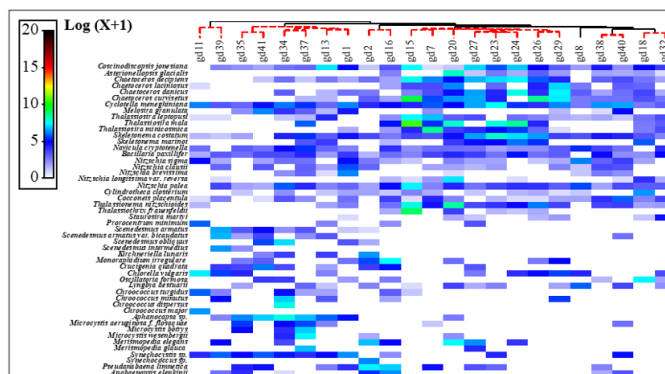


Figure 3 Shade plot, a visual representation abundances of a total of 50 phytoplankton species out of 710 phytoplankton taxa across different stations during wet season with spectrum scale intensity proportional to the Log X + 1 abundance. The dendrogram shows species clustering using standard agglomerative methods of calculating group average, with white denotes the absence of the species.

The phytoplankton wet biomass fluctuated across the mangroves, with a mean value of $2.23 \times 10^4 \text{ mgL}^{-1}$, Figure S3 (supplementary material), and ranged from $3.80 \times 10^3 \text{ mgL}^{-1}$ to $8.40 \times 10^4 \text{ mgL}^{-1}$. It was significantly different ($t = 2.16, p = 0.05$) across the mangroves. The algal biomass for all stations was higher in the Coscinodiscophyceae

compared to the other Classes of phytoplankton (Figure 4b). Meanwhile, there was an increased biomass of Mediophyceae (gd-7, 20 & 29); Bacillariophyceae (gd-8, 11, 16 & 35); Chlorophyceae (gd-34 & 41); Trebouxiophyceae (gd-11), and Cyanophyceae (gd-2).

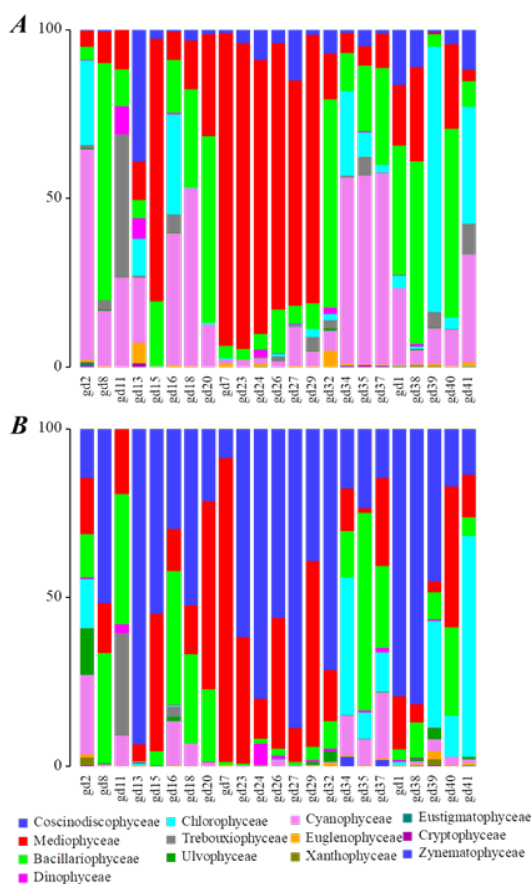


Figure 4 Spatial distribution of Algal abundance (A) and Biomass (B) at different phytoplankton Classes.

Phytoplankton size distribution

The cell size range was 0.8-306 μm and was grouped into four different size volumes, Figure 5. The phytoplankton class size of < 100 μm³ were mainly predominated by *Scenedesmus* sp., *Monoraphidium* sp., *Selenastrum* sp., *Crucigenia* sp., *Merimopodia* sp., *Chroococcus* sp., *Microcystis* sp., *Synechococcus* sp., *Aphanocapsa* sp., *Kirchneriella* sp., *T. mala*, *N. closterium* f. *minutissima*, *N. atomus*, *Leptocylindrus minimus*, etc, which were recorded across gd-2, 15, 16, 34, 35, 37, 39 & 41. Their distribution and proliferation in the mangroves were associated with high EC and nutrient salts. Class size 100-250 μm³ was maximally represented at gd-11. *C. vulgaris*, *N. palea*, *C. major*, *C. turgidus*, and *Scenedesmus* sp. were the predominant species of this class. However, these two class size were mainly freshwater taxa that were added to the mangroves via river water input and occurred only at low salinity sites. The class size 250-1000 μm³ was maximally represented by *C. curvisetus* at gd-26. Other species that make up this class include *P. limnetica*, *H. tenerrima*, *S. marinoi*, *N. transitans*, *N. cryptotenella*, *N. brevissima*, etc. The class size > 1000 μm³ constitute the greater proportion of phytoplankton assemblage in the mangroves. Its distribution fluctuated across the mangroves but was mainly represented across the Leizhou Peninsular. Species, such as *Coscinodiscopsis* sp., *Chaetoceros* sp., *C. meneghiniana*, *Thalassiosira* sp., *S. costatum*, *O. sinensis*, *B. paxillifer*, *N. longissima* var. *reversa*, *Thalassionema* sp., *Thalassiothrix* sp., *O. formosa*, *L. aestuarii*, etc predominated this class. Generally, class size > 1000 μm³ constituted the largest phytoplankton biomass.

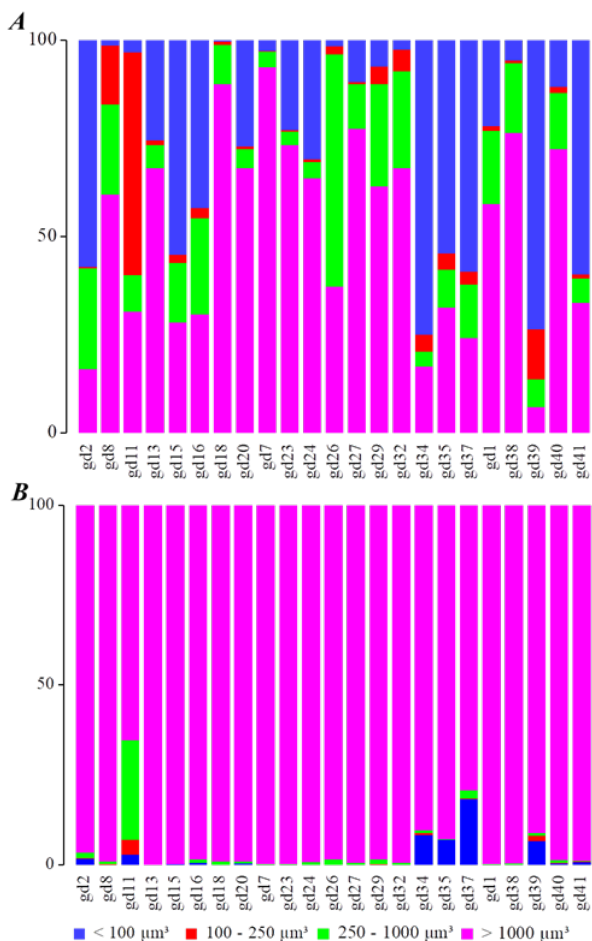


Figure 5 Phytoplankton size volume distribution: (A) size class abundance and (B) biomass distribution.

Multivariate analysis of the phytoplankton community structure

The hierarchical clustering amongst phytoplankton abundance at 50% similarity showed four groups; each was clearly associated with a specific site (Figure 6). The clustering dendrogram displayed a strong inter-relation with high similarities within groups of similar species on specific sites (Table 2). Diatoms formed the highest percentage contribution in a cluster 'b & c' compared to other phytoplankton groups, with the occurrence of *C. meneghiniana*, *C. decipiens*, *S. costatum*, *C. curvisetus*, *C. danicus*, *N. palea*, *C. jonesiana*, *T. minicosmica*, *T. leptopus*, *T. mala*, and *T. nitzschioides* predominating the Leizhou Peninsular (Figure 6). Periphytic and planktonic cyanobacteria (*Aphanocapsa* sp. and *Synechocystis* sp. respectively) with other diatom species (*C. meneghiniana*, *C. jonesiana* and *N. palea*) contributed to the intra-site species similarity within cluster 'd' which is associated with low salinity and high EC. Within cluster 'a', species such as *P. limnetica*, *M. irregular*, *M. elegans*, and *C. meneghiniana* contributed to the intra-site species similarity and were associated with high EC and nutrient salts.

Table 2 SIMPER analysis. The most contributing species of intra-site similarities are reported with their average similarity (Av. Sim) and percentage of contribution to the average intra-group similarity (%)

Group a		Group b	
Species	SIM (%)	Species	SIM %
<i>Pseudanabaena limnetica</i>	22.67	<i>Chaetoceros decipiens</i>	10.72
<i>Monoraphidium irregulare</i>	18.43	<i>Cyclotella meneghiniana</i>	9.69
<i>Merismopodia elegans</i>	15.84	<i>Skeletonema costatum</i>	8.23
<i>Cyclotella meneghiniana</i>	13.6	<i>Thalassionema nitzschioides</i>	7.89
<i>Skeletonema costatum</i>	8.36	<i>Thalassiosira mala</i>	7.71
<i>Chaetoceros decipiens</i>	5.84	<i>Chaetoceros curvisetus</i>	7.56
<i>Chaetoceros curvisetus</i>	5.84	<i>Thalassiosira minicosmica</i>	7.43
<i>Nitzschia palea</i>	5.84	<i>Chaetoceros danicus</i>	6.76
<i>Coscinodiscopsis jonesiana</i>	3.58	<i>Odontella sinensis</i>	4.68
Total	100	Total	70.67
Av. Sim	57.19	Av. Sim	65.52
Group c		Group d	
Species	SIM %	Species	SIM %
<i>Cyclotella meneghiniana</i>	12.95	<i>Synechocystis</i> sp.	22.16
<i>Skeletonema costatum</i>	12.02	<i>Cyclotella meneghiniana</i>	18.41
<i>Chaetoceros curvisetus</i>	10.56	<i>Aphanocapsa</i> sp.	15.85
<i>Nitzschia palea</i>	10.48	<i>Coscinodiscopsis jonesiana</i>	7.77
<i>Coscinodiscopsis jonesiana</i>	10.21	<i>Nitzschia palea</i>	7.38
<i>Chaetoceros danicus</i>	8.51	<i>Skeletonema costatum</i>	6.68
<i>Chaetoceros decipiens</i>	5.80	<i>Chlorella vulgaris</i>	4.60
<i>Thalassiosira leptopus</i>	5.72	<i>Pseudanabaena limnetica</i>	3.46
<i>Thalassionema nitzschioides</i>	5.62	<i>Chaetoceros decipiens</i>	1.88
<i>Chaetoceros lacinosus</i>	3.99	<i>Microcystis botrys</i>	1.82
Total	85.86	Total	90.01
Av. Sim	57.72	Av. Sim	48.42

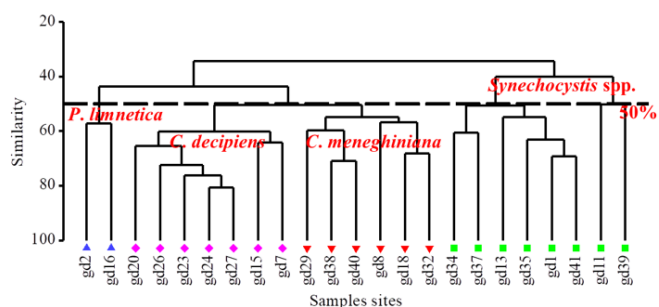


Figure 6 Hierarchical clustering of dendrogram showing dominant species in various clusters (group-average linking 23 phytoplankton samples of Bray Curtis similarities calculated on Log (X+1) transformed abundance).

The results of MDS ordinations of samples based on Log (x + 1) transformed abundance data are shown in Figure 7. By superimposing the sites based on similarity tests, 4 main groups have been formed in the mangroves. It becomes apparent that the groups differ in community composition, as respective sites group together. This is supported by the significantly lower stress factor of the ordination (0.14). Group site ‘b & c’ was dominated by planktonic diatom species whose class size ranged from 250 to < 1000 μm³. They were mainly marine residents, confirming the presence of neritic-rich water biota in the mangroves. In contrast, the group site ‘d’ was dominated by planktonic and periphytic cyanobacteria whose class size was < 100 μm³. They were mainly fresh-water residents and occupied the eastern part of the Guangdong coast. The inter-site dissimilarity (> 60%) between ‘b & d’ and ‘c & d’ was mainly caused by marine diatoms and planktonic cyanobacteria respectively. The ANOSIM test (global R = 0.825; p = 0.1) and pairwise tests (Table S4) further explain the similarity level in species composition and distribution among the sites, and between the various groups.

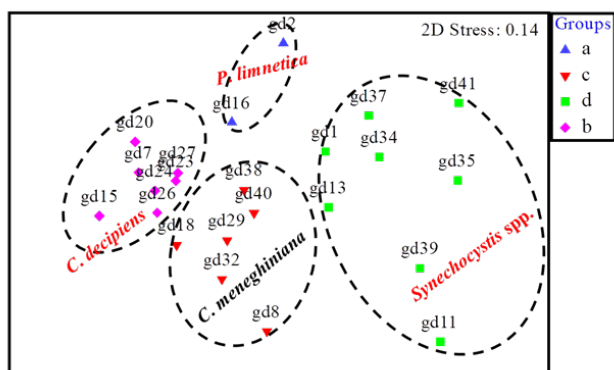


Figure 7 MDS ordinations of the phytoplankton samples based on Log (X+1) transformed abundance data and Bray-Curtis similarities showing dominant species in various clusters.

Table 3 Results of Pearson’s correlation coefficient between physicochemical variables and phytoplankton taxa in the mangrove forest

Phytoplankton taxa	Codes	pH	Sali.	Turb	Tem	EC	Phos	Nitra	Nitri	Silic
Diatom										
<i>C. jonesiana</i>	Cojo	0.152	0.367	-0.135	-0.258	0.124	-0.023	-0.312	-0.313	-0.155
<i>A. glacialis</i>	Aagl	0.332	0.286	-0.281	-0.347	-0.378	-0.175	-0.196	-0.200	0.079
<i>C. decipiens</i>	Chde	0.447*	0.579**	-0.097	0.011	-0.188	-0.071	-0.140	-0.151	-0.342
<i>C. danicus</i>	Chda	0.495*	0.473*	0.086	-0.061	-0.236	-0.075	-0.155	-0.173	-0.034
<i>C. curvisetus</i>	Chcu	0.573**	0.575**	-0.320	0.091	-0.337	-0.117	-0.116	-0.133	-0.347
<i>C. meneghiniana</i>	Cyme	0.056	0.240	-0.157	0.283	0.260	-0.001	-0.111	-0.108	0.016

The relationship between environmental variables and phytoplankton taxa

The relationship between environmental parameters and the phytoplankton characteristics was modeled using the CCA ordination plot and Pearson’s correlation analysis. Here, a relationship was established between phytoplankton class size and the environmental parameters (Table 3). The statistical relationships between cell abundance of phytoplankton taxa and environmental variables are shown in Figure 8 and Table S5. The canonical axes of phytoplankton taxa/environmental variables significantly accounted for 68.88% (*pseudo-F* = 0.662, *p* < 0.002), which axis 1 and 2 explained 51.35% and 17.53% of the variation respectively. This explains the fact that the phytoplankton taxa were significantly related to environmental variables on each axis. Furthermore, the occurrence and distribution of small-celled species of green algae, cyanobacteria, and diatoms were positively influenced by EC and nitrate. Most of these taxa were riverine assemblages and constituted the main food source for copepod zooplankton. The distribution of large-celled size diatoms and dinoflagellates was positively affected by pH, salinity concentration, and nutrients. Meanwhile, phytoplankton has special ecophysiological traits and each species tends to become dominant when growth conditions match its specific requirements. In our study, *A. glacialis*, *T. leptopus*, *T. mala*, *T. minicosmica*, *C. jonesiana*, *Chaetoceros* sp., *S. costatum*, *T. nitzschioides*, *M. irregular*, *S. obliquus*, and *P. limneticus* could become an indicator for nutrient enrichments as they become dominant. Specifically, *T. mala* formed a negative correlation with nutrients, while *T. leptopus*, *S. costatum*, *T. nitzschioides*, *M. wesenbergii*, *M. botrys*, *M. elegans*, *M. irregular*, *S. obliquus* and *P. limnetica* showed a significant positive correlation with nutrients. The massive proliferation of these taxa was mainly affected by nutrient fluctuations than were closely related to temperature changes.

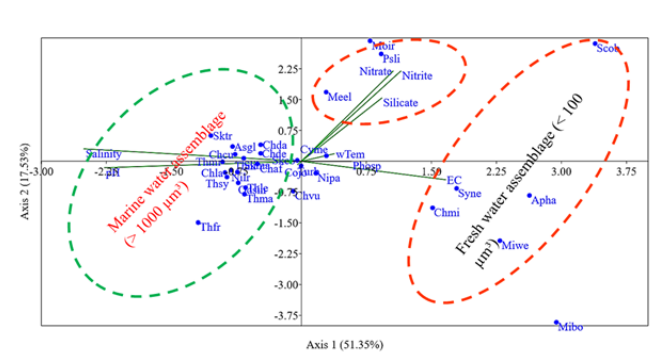


Figure 8 CCA showing the relationship between phytoplankton assemblages, class size and environmental variables.

Table 3 Continued...

Phytoplankton taxa	Codes	pH	Sali.	Turb	Tem	EC	Phos	Nitra	Nitri	Silic
Diatom										
<i>T. leptopus</i>	Thle	0.437*	0.445*	0.198	0.097	-0.309	-0.133	-0.318	-0.324	-0.520*
<i>T. mala</i>	Thma	0.337	0.334	-0.170	-0.180	-0.105	0.022	-0.233	-0.237	-0.427*
<i>T. minicosmica</i>	Thmi	0.586**	0.450*	0.028	-0.083	-0.191	-0.306	-0.247	-0.251	-0.389
<i>S. costatum</i>	Skco	0.267	0.390	-0.304	-0.202	-0.054	-0.197	-0.271	-0.301	-0.209
<i>T. nitzschoides</i>	Thni	0.521*	0.597**	-0.035	-0.046	-0.250	-0.125	-0.333	-0.338	-0.373
<i>T. frauenfeldii</i>	Thfr	0.266	0.298	-0.140	-0.036	-0.058	0.112	-0.123	-0.125	-0.471*
<i>C. lacinosus</i>	Chla	0.549**	0.431*	-0.095	0.138	-0.325	-0.066	-0.237	-0.241	-0.134
<i>C. affinis</i>	Chaf	0.365	0.344	-0.071	-0.033	-0.112	-0.328	-0.253	-0.257	-0.259
<i>S. marinoi</i>	Skma	0.349	0.227	-0.274	-0.634**	-0.287	-0.092	-0.223	-0.227	-0.005
<i>S. tropicum</i>	Sktr	0.451*	0.403	-0.308	-0.479*	-0.166	-0.104	-0.187	-0.191	0.000
<i>O. sinensis</i>	Odsin	0.513*	0.471*	0.026	0.081	-0.175	-0.285	-0.292	-0.297	-0.635**
<i>N. longissima var. reversa</i>	Nilr	0.337	-0.001	-0.002	-0.402	-0.533**	-0.118	-0.150	-0.153	0.053
<i>N. palea</i>	Nipa	0.182	0.141	-0.052	-0.034	0.157	-0.126	-0.319	-0.326	-0.331
<i>T. synedriforme</i>	Thsy	0.330	.371	-0.165	-0.069	0.127	-0.032	-0.155	-0.158	-0.365
Green algae										
<i>M. irregulare</i>	Moir	-0.185	-0.001	-0.240	0.004	0.019	0.041	0.459*	0.451*	0.395
<i>C. vulgaris</i>	Chvu	0.160	0.125	0.202	-0.007	0.016	-0.021	-0.243	-0.247	-0.203
<i>S. obliquus</i>	Scob	-0.403	-0.506*	0.188	0.147	0.505*	0.012	0.381	0.416*	0.445*
Cyanobacteria										
<i>Aphanocapsa sp.</i>	Apha	-0.674**	-0.806**	-0.013	0.040	0.526**	0.030	0.084	0.118	0.182
<i>M. elegans</i>	Meel	-0.076	-0.114	-0.219	-0.302	-0.303	-0.128	0.292	0.262	0.060
<i>P. limnetica</i>	Psli	-0.270	-0.097	-0.244	0.091	0.020	-0.130	0.558**	0.553**	0.231
<i>C. minutus</i>	Chmi	-0.320	-0.233	0.096	0.242	0.247	-0.014	-0.144	-0.147	0.185
<i>M. botrys</i>	Mibo	-0.0500*	-0.601**	-0.241	-0.101	0.387	0.189	-0.113	-0.115	-0.062
<i>M. wesenbergii</i>	Miwe	-0.405	-0.491*	-0.284	-0.041	0.148	0.146	0.055	0.044	0.011
<i>Synechocystis sp.</i>	Syne	-0.613**	-0.622**	0.012	0.157	0.570**	-0.024	-0.005	0.026	0.092

*. Correlation is significant at the 0.05 level (2-tailed). **. Correlation is significant at the 0.01 level (2-tailed). {EC. electrical conductivity, Sali. salinity, Turb. turbidity, Tem. water temperature, Phosp. phosphate, Nitra. Nitrate, Nitri. Nitrite, Silic. Silicate}.

Discussion

Mangroves usually maintain relatively high phytoplankton production due to naturally available nutrients from the surrounding mangrove litters which sustain the ecological balance between phytoplankton productivity and diversity.^{37,38} According to Tanaka and Choo,³⁹ nutrient out-welling from the mangrove swamp affected the phytoplankton distribution. Meanwhile, nutrient inputs from anthropogenic activities into the mangroves often offset its fragile ecological balance, resulting in eutrophication. In this study, higher phytoplankton densities (Figure S4) coincide with higher phosphate availability, illustrating the relationship between phytoplankton and environmental changes, especially those related to eutrophication. Moreover, the pca biplot analysis has revealed the main nutrient salt that impacted the phytoplankton community structure in the mangroves. Studies have shown that high phytoplankton density in mangrove estuaries is generally controlled by phosphate and nitrogen concentration.^{5,6,13,34,40} The spatial fluctuation of nutrient concentrations in the mangroves could be due to the monsoonal intrusion of rainfall along with land runoff^{16,41} from urban areas, agricultural farmlands, waste water discharge from aquaculture facilities,^{6,39,40} influxes from the sediments,^{39,43} oxidation of ammonia and biodegradation of detrital material,¹⁶ and utilization by the mangrove plants⁴³ and algal cells.⁵ Generally, nitrate, phosphates, salinity, and turbidity have a positive correlation with the abundance and distribution of phytoplankton in tropical ecosystems.^{5,14,44}

Species dominance and richness in the mangroves depend on environmental variables that would provide a competitive advantage to the specific group. Under natural conditions, diatoms normally contribute the highest percentage compared to other phytoplankton

groups.^{5,6,34} In this study, diatoms dominated the phytoplankton community (71.90%) but cyanobacteria and green algae formed only 16.35% and 10.70% respectively of the total phytoplankton when environmental variables favored them. Dinoflagellates formed <0.5% of the total phytoplankton species. Diatoms dominated the phytoplankton composition in mangrove estuaries and were influenced by increase pH, salinity, and silicate concentration,^{6,34,45} whereas cyanobacteria and green algae were influenced by low salinity and high EC and nutrients concentration.⁶ As indicated by the PCA analysis, turbidity, EC, salinity, water temperature, and nitrite were the main factors influencing the phytoplankton community structure in the mangroves. Meanwhile, the inputs of freshwater showed impact on the salinity gradient, which, together with the increased water turbidity, subsequently caused a decline in diatom abundance and favored cyanobacteria and green algae increase. In fact, salinity has been reported as a major factor associated with shifts in plankton community structure in the mangroves.^{5,6,14,16,31,44,46}

Phytoplankton size distribution as a function of nutrient availability in the study area has been observed. However, nutrient enrichment alters phytoplankton community composition and distribution in coastal waters.⁴⁷ No consistent model relationship between eutrophy and phytoplankton size distributions was established, though Walters et al.⁴⁸ and Kiorboe⁴⁹ reported that increased nutrient concentrations increased relatively larger cells in phytoplankton populations. Kimor⁵⁰ and Huszar et al. suggested that small phytoplankton cells will dominate under conditions of eutrophication. In this study, the dominance of small size taxa was marked by average to a high concentration of phosphate in the water. Generally, the spatial distribution of phytoplankton class sizes across the study area was found to be characterized by nutrient characteristics and salinity/

freshwater gradient. The result of CCA exhibits that algal biomass of different sizes is associated differently with the environmental variables. The test of significance using the Monte Carlo test on CCA highlights the linear relationship between phytoplankton species-environmental variable relations ($p < 0.05$), (Table S6). The eigenvalues and the percentages of variance on axis 1 are found to be higher than axis 2.^{22,51} We found that taxon biomass of a size range of $250 > 1000\mu\text{m}^3$ correlated positively significantly with pH and salinity, and negatively with nutrients. Meanwhile, the taxon biomass of size range of $< 250\mu\text{m}^3$ correlated positively significantly with EC and nutrients. This class size formed the main food source of copepod during this period. Based on this study, we discover that the class size/

nutrient relationship in mangroves is influenced by salinity/freshwater gradient and nutrients.

Phytoplankton richness across the mangrove was $7.31 \geq d \leq 20.63$ indicating a healthy ecosystem (Table S6). However, the positive significant correlation that exists between Simpson's diversity index ($1-\lambda$), Shannon diversity index and species richness ($p < 0.01$) indicated that the variation of species diversity in the mangroves coincide with species richness.⁴⁰ Comparing the species diversity in this study with other mangroves (Table 4), it's observed that the species diversity at the Guangdong mangrove ecosystems remains richest. Rare and less common taxa constitute the greatest proportion of algal assemblage in the mangroves and may need better conservation practices.

Tables 4 Phytoplankton abundance, diversity and biomass at different mangrove ecosystem

Estuary/region	Phytoplankton Abundance/ Species Richness	Chlorophyll A	Biomass (wet weight)	Source
Matang mangrove estuary, Malaysia	NA	$< 20 \mu\text{g.L}^{-1}$ (neap tide); $80 \mu\text{g.L}^{-1}$ (spring tide)	NA	Tanaka and Choo (2000)
Godavari mangrove estuary, India	NA	$12.49 \mu\text{g.L}^{-1}$	NA	Tripathy et al., (2005)
Pichavaram mangrove waters, India	$1400 - 292,000 \text{ cells.L}^{-1}$; $750 - 321,000$ cells.L^{-1} ; $400 - 297,000 \text{ cells.L}^{-1}$ in different locations	$0.24 - 69.82 \mu\text{g.L}^{-1}$; $0.20 - 105.60$ $\mu\text{g.L}^{-1}$; $0.20 - 94.80 \mu\text{g.L}^{-1}$ in different locations	NA	Rajkumar et al., (2009)
Kaduviya estuary, Nagapattinam, India	$28,797 - 62,900 \text{ cells.L}^{-1}$; $14,135-74,697 \text{ cells.L}^{-1}$ in different locations	$3.4 - 9.3 \mu\text{g.L}^{-1}$	NA	Perumal et al., (2009)
Sundarbans mangrove forest, Bangladesh	36 species	NA	NA	Aziz et al., (2012)
Kuantan, Pahang, Malaysia	71 species; $7.0 \times 10^4 \text{ cells.L}^{-1}$	NA	NA	Mohammad-Noor et al., (2013)
Mangrove estuary, Philippines	61 species	$0.02 - 2.6 \mu\text{g.L}^{-1}$	NA	Canini et al., (2013)
Sundarbans mangrove estuaries, Bangladesh	$3.755 \times 10^3 - 10^5 \text{ cells.L}^{-1}$	$0.24 - 3.11 \mu\text{g.L}^{-1}$	NA	Rahman et al., (2013)
Kuala Nyalau river estuary, Malaysia	$113,000 - 147,000 \text{ cells.L}^{-1}$	$0.12 - 0.18 \text{ mg.m}^{-3}$	NA	Saifullah et al., (2014)
Eastern Obolo mangrove estuary, Nigeria	Dry season: 84 species, 6959 algal unit; Wet season: 84 species, 4027 algal unit	Dry season: $0.002 - 0.01 \text{ mg.L}^{-1}$, Wet season: $0.002 - 0.02 \text{ mg.L}^{-1}$	NA	Effiong et al., (2016)
South China Sea mangrove ecosystem along Guangdong coast	Wet season: 671 species, 12.56×10^7 cells.L^{-1}	Wet season: $0.14 - 13.53 \text{ mg.m}^{-3}$	Wet season 5.13×10^5 mg.L^{-1}	This study

Conclusion

This study elucidated that the tropical phytoplankton community structure in the mangroves were mainly shaped by environmental fluctuations associated with the rainy season. Diatoms formed the most dominant group, contributing to 71.90% of the total phytoplankton and generating the largest algal biomass in the mangrove ecosystems. Cyanobacteria and green algae formed the next largest group of phytoplankton in the mangroves. The main driving factors influencing the spatial dynamics of phytoplankton species were rainfall, tidal mixing, nutrients, water temperature, turbidity, and EC. The phytoplankton community structure in the study area was characterized by an indicator species associated with catchment characteristics. *C. meneghiniana*, *S. costatum*, *Chaetoceros* sp., *N. palea*, *C. jonesiana*, *T. nitzschoides*, and *Thalassiosira* spp. were dominant in the Leizhou Peninsular characterized by high

salinity, pH, and average nutrients. There was a shift in dominance from diatoms to *P. limneticus*, *M. irregularis*, *Microcystis* sp., *S. obliquus*, *Aphanocapsa* sp., *Chroococcus* sp., etc. at the site where salinity and pH were low while EC and nutrients remained high. An algae cell size/nutrient relationship was established in the mangroves. The small-sized taxa, which were mainly of fresh-water origin, were controlled by high nutrients and EC, whereas the large-sized species were mainly characterized by moderate nutrients, high salinity, and pH. Diatoms and some periphytic cyanobacteria tend to form the bulk of the biomass in this category. Biodiversity community structures revealed that the study area maintains the highest species richness and diversity among the mangrove ecosystems in the world. Further studies are needed to model the selection of phytoplankton species for various environmental conditions and the cell size/nutrient association in the mangrove ecosystems.

Acknowledgement

This research was supported by the National Nature Science Foundation of China (No. 41676086). The authors appreciate the assistance given by Prof. Wang You-Shao, Prof. Cheng Hao and other members of the Mangrove Research Team during the studies.

Declaration of competing interest

The author declares that there is no known competing financial interests or personal relationships that could have appeared to influence the work reported in this paper.

References

- Khan TA. Limnology of four saline lakes in western Victoria, Australia. *Limnologia*. 2003;33(4):327-339.
- Cloern JE, Jassby AD. Patterns and scales of phytoplankton variability in estuarine coastal ecosystems. *Estuaries and Coasts*. 2010;33:230-241.
- Field CB, Behrenfeld MJ, Randerson JT, et al. Primary production of the biosphere: integrating terrestrial and oceanic components. *Science*. 1998;281(5374):237-240.
- Sin Y, Wetzel LR, Anderson CI. Spatial and temporal characteristic of nutrient and phytoplankton dynamics In the York River Estuary, Virginia. Analysis of long-term data. *Estuaries*. 1999;22(2):260-275.
- Inyang AI, Wu ML, Antai EE, et al. Shifts in species dominance related to spatial assemblages and variation in environmental parameters in a tropical mangrove estuary. *Marine Environmental Research*. 2023;191:106173.
- Inyang AI, Wang YS. Phytoplankton diversity and community responses to physicochemical variables in mangrove zones of Guangzhou Province, China. *Ecotoxicology*. 2020;29:650-668.
- Madhu NV, Jyothibabu R, Balachandran KK, et al. Monsoonal impact on planktonic standing stock and abundance in a tropical estuary (Cochin Backwaters—India). *Estuar Coast Shelf Sci*. 2007;73(1-2):54-64.
- Durate P, Macedo MF, Da Fonseca LC. The relationship between phytoplankton diversity and community function in a coastal lagoon. *Hydrobiologia*. 2006;183:3-18.
- Inyang AI, Dan MU, Sunday KE. Seasonal and Spatial Variations of Physicochemical Properties of Eastern Obolo Coastal Water, Niger Delta-Nigeria. *Mar Biol Oceanogr*. 2018;7:1.
- Inyang AI, Zhou Y, Wang YS. Characteristics of water quality and its eutrophication assessment in mangrove ecosystems along the Guangdong coast. *Journal of Tropical Oceanography*. 2021;10:1020-1035.
- Hou Z, Jiang Y, Liu Q, et al. Impacts of Environmental Variables on a Phytoplankton Community: A Case Study of the Tributaries of a Subtropical River, Southern China. *Water*. 2018;10:152.
- Kjørboe T. *Material flux in the water column*. In: Richardson and Jørgensen, editors. *Eutrophication in Coastal Marine Ecosystems, Coastal and Estuarine Studies 52*. American Geophysical Union, Washington, D.C. 1996. P. 167-194.
- Rahaman SMB, Sarder L, Rahaman MS, et al. Nutrient dynamics in the Sundarbans mangrove estuarine system of Bangladesh under different weather and tidal cycles. *Ecological Processes*. 2013a;2(29):1-13.
- Saifullah ASM, Kamal AHM, Idris MH, et al. Phytoplankton in tropical mangrove estuaries: role and interdependency. *Forest Science and Technology*. 2016;12(2):104-113.
- Brito AC, Silva T, Beltrán C, et al. Phytoplankton in two tropical mangroves of São Tomé Island (Gulf of Guinea): A contribution towards sustainable management strategies. *Regional Studies in Marine Science*. 2017;9:89-96.
- Vajravelu M, Martin Y, Ayyappan S, et al. Seasonal influence of physico-chemical parameters on phytoplankton diversity, community structure and abundance at Parangipettai coastal waters, Bay of Bengal, South East Coast of India. *Oceanologia*. 2017;60:114-127.
- Achary MS, Panigrahi S, Satpathy KK, et al. Nutrient dynamics and seasonal variation of phytoplankton assemblages in the coastal waters of southwest Bay of Bengal. *Environ Monit Assess*. 2014;186:5681-5695.
- Chu TV, Torretton JP, Mari X, et al. Nutrient ratios and the complex structure of phytoplankton communities in a highly turbid estuary of Southeast Asia. *Environ Monit Assess*. 2014;186:8555-8572.
- Wang HH, Song SH, Qi YZ. A comparative study of phytoneuston and the phytoplankton community structure in Daya Bay, South China Sea. *J Sea Res*. 2014;85:474-482.
- Sun CC, Wang YS, Sun S, et al. Dynamic analysis of phytoplankton community characteristics in Daya Bay, China. *Acta Ecol Sin*. 2006;26:3948-3958.
- Qu HJ, Kroeze C. Past and future trends in nutrients export by rivers to the coastal waters of China. *Sci. Total Environ*. 2010;408:2075-2086.
- Liu C, Liu L, Shen H. Seasonal variations of phytoplankton community structure in relation to physico-chemical factors in Lake Baiyangdian, China. *Procedia Environ Sci*. 2010;2:1622-1631.
- Nguyen LTT, Mosestrup O, Daugbjerg N. Planktic cyanobacteria from freshwater localities in Thuathien-Hue province, Vietnam. III. Phylogenetic inference based on partial phycocyanin sequences, morphological and toxicological characters. *Algalogical studies*. 2014;144:19-43.
- Felisberto SA, da Silva e Souza DB. Characteristics and Diversity of Cyanobacteria in Periphyton from Lentic Tropical Ecosystem, Brazil. *Advances in Microbiology*. 2014;4:1076-1087.
- Li Y, Zhao Q, Lü S. The genus *Thalassiosira* off the Guangdong coast, South China Sea. *Botanica Marina*. 2013;56(1):83-110.
- Newell GB, Newell RC. *Marine Plankton: A Practical Guide*. Hutchinson and Company Publishers Ltd. London. 1977:229pp.
- Guiry MD, Guiry GM. *Alga eBase*. World-wide electronic publication, National University of Ireland, Galway. 2020.
- Olenina I, Hajdu S, Edler L, et al. *Biovolumes and size-classes of phytoplankton in the Baltic Sea*. HELCOM Baltic Sea Environmental Proceedings No 106. 2006.
- Sun J, Liu D. Geometric models for calculating cell biovolume and surface area for phytoplankton. *Journal of Phytoplankton Research*. 2003;25:1331-1346.
- Cen. *DIN EN 16695 Water quality – guidance on the estimation of phytoplankton biovolume: English version EN 16695*. 2015.
- Snoeijs P, Busse S, Potapova M. The importance of diatom cell size in community analysis. *Journal of Phycology*. 2002;38:265-272.
- Sundbäck K. *Microphytobenthos on sand in shallow brackish water, Öresund, Sweden*. Primary production, Chlorophyll a content and species composition (diatoms) in relation to some ecological factors. Ph.D. thesis, Lund University. 1983.
- HELCOM. Guidelines concerning phytoplankton species composition, abundance and biomass. Manual for Marine Monitoring in the COMBINE Programme of HELCOM. Annex C-6. 2015.
- Hilaluddin F, Yusoff F Md, TodaT. Shifts in diatom dominance associated with seasonal changes in an estuarine-mangrove phytoplankton community. *J Mar Sci Eng*. 2020;8:528-547.
- Clarke KR, Warwick RM. *Change in Marine Communities: An Approach to Statistical Analysis and Interpretation*. PRIMER-E, Plymouth, UK. 2001.

36. Clarke KR, Gorley RN. *PRIMER v6: User manual/tutorial*. PRIMER-E, Plymouth, UK. 2006.
37. Aké-Castillo JA, Vázquez G. Phytoplankton variation and its relation to nutrients and allochthonous organic matter in a coastal lagoon on the Gulf of Mexico. *Estuar Coast Shelf Sci*. 2008;78:705–714.
38. Rahaman SMB, Golder J, Rahaman MS, et al. Spatial and Temporal Variations in Phytoplankton Abundance and Species Diversity in the Sundarbans Mangrove Forest of Bangladesh. *Int J Mar Sci*. 2013b;3(2):126.
39. Tanaka K, Choo PS. Influence of nutrient outwelling from the mangrove swamp on the distribution of phytoplankton in the Matang mangrove estuary, Malaysia. *J Oceanogr*. 2000;56:69–78.
40. Manna S, Chaudhuri K, Bhattacharyya S, et al. Dynamics of Sundarban estuarine ecosystem: Eutrophication induced threat to mangroves. *Saline Syst*. 2010;6:8.
41. Satpathy KK, Mohanty AK, Natesan U, et al. Seasonal variation in physico – chemical properties of coastal water of Kalpakkam East Coast of India with special emphasis on nutrients. *Environmental Monitoring and Assessment*. 2009;164:153–171.
42. Temino-Boes R, Romero-López R, Romero I. A Spatiotemporal Analysis of Nitrogen Pollution in a Coastal Region with Mangroves of the Southern Gulf of Mexico. *Water*. 2019;11:21–43.
43. Krumme U, Herbeck LS, Wang T. Tide- and rainfall-induced variations of physical and chemical parameters in a mangrove-depleted estuary of East Hainan (South China Sea). *Marine Environmental Research*. 2012;82:28–39.
44. Inyang AI, Effiong KS. Spatial Distribution of Diatoms and Nutrients in a Mangrove Swamp of Eastern Obolo, Niger Delta. *Journal of Scientific Research & Reports*. 2016;12(3):1-17.
45. Donald HK, Foster GL, Fröhberg N, et al. The pH dependency of the boron isotopic composition of diatom opal (*Thalassiosira weissflogii*). *Biogeochemistry*. 2020;17:2825–2837.
46. Nursuhayati AS, Yusoff FM, Shariff M. Spatial and temporal distribution of phytoplankton in Perak estuary, Malaysia, during monsoon season. *J Fish Aquat Sci*. 2013;8:480–493.
47. Lassen MF, Brammi ME, Richardson K, et al. Phytoplankton community composition and size distribution in the Langat River Estuary, Malaysia. *Estuaries*. 2004;27:716–727.
48. Walters CJ, Park RA, Koonce JF. *Dynamic models of lakes ecosystems*, In: ED Le Cren and RH Lowe-McConnell, editors. *The Functioning of Fresh Water Ecosystems*. Cambridge University Press, Cambridge, England. 1980. p. 455-579.
49. Kiørboe T. Turbulence, phytoplankton cell size, and the structure of pelagic food webs. *Advances in Marine Biology*. 1993;29:1-72.
50. Kimor B. *The impact of eutrophication on phytoplankton composition in coastal marine ecosystems*, In: RAWollenweider, R Marchetti, R Viviani, editors. *Marine Coastal Eutrophication: The Response of Marine Transitional Systems to Human Impact: Problems and Perspectives for Restoration*. Proceedings of an International Conference, Bologna, Italy, 21-24 March 1990. Elsevier, Amsterdam, The Netherlands. 1992. p. 871-878.
51. Sharma RC, Singh N, Chauhan A. The influence of physicochemical parameters on phytoplankton distribution in a head water stream of Garhwal Himalayas: a case study. Egypt. *J Aquat Res*. 2016;42:11–21.